Fabrication of a quantum well heterostructure based on plasma polymerized aniline and its characterization using STM/STS

2009 J. Phys. D: Appl. Phys. 42 165309

(http://iopscience.iop.org/0022-3727/42/16/165309)

J. Phys. D: Appl. Phys. **42** (2009) 165309 (7pp) doi:10.1088/0022-3727/42/16/165309

Fabrication of a quantum well heterostructure based on plasma polymerized aniline and its characterization using STM/STS

T N Narayanan[1], Soumya Jose[1], Senoy Thomas[1], S H Al-Harthi[2] and M R Anantharaman[1,3]

[1] Department of Physics, Cochin University of Science and Technology, Cochin-22, Kerala, India
[2] Department of Physics, College of Science, Sultan Qaboos University, Muscat, Oman

E-mail: mraiyer@yahoo.com

Received 26 April 2009, in final form 6 July 2009
Published 31 July 2009
Online at stacks.iop.org/JPhysD/42/165309

Abstract
Two-dimensional electronic systems play a crucial role in modern electronics and offer a multitude of opportunities to study the fundamental phenomena at low dimensional physics. A quantum well heterostructure based on polyaniline (P) and iodine doped polyaniline (I) thin films were fabricated using radio frequency plasma polymerization on indium tin oxide coated glass plate. Scanning probe microscopy and scanning electron microscopy studies were employed to study the morphology and roughness of the polymer thin films. Local electronic density of states (LDOS) of the P–I–P heterostructures is probed using scanning tunnelling spectroscopy (STS). A step like LDOS is observed in the P–I–P heterostructure and is attributed to the quantum well confinement of electrons in the polymer heterostructure.

(Some figures in this article are in colour only in the electronic version)

1. Introduction

Recent progress in material science provides an opportunity for the fabrication of various artificial structures of nanometre sizes. Remarkable developments in nanotechnology in the past decades have almost reached the fundamental physical limits and the miniaturization threshold for electronic devices made of conventional semiconductors. This has accelerated the interest in nanostructured organic materials and devices which have the ability to control their properties on a molecular level [1, 2]. Conducting polymer nanostructures combine the advantages of organic conductors and low dimensional systems and therefore should yield many interesting physicochemical properties and useful applications.

Conducting polymers can respond to various external stimuli and hence represent a new class of 'intelligent materials' [3]. The unique optical and electronic properties of conducting polymers qualify them to become ideal materials for various technological applications such as light emitting diodes [4], nonlinear optical devices [5], field effect transistors [6] and flat panel displays [7, 8].

Polyaniline (PANI) occupies a distinctive position in this category and is identified as a potential material with excellent electrical and optical properties and high environmental stability [9]. The ability to control the physical properties of polyaniline and the inherent stability of polyaniline thin films (P) make PANI an ingenious member suited for various optoelectronic device fabrications [10]. Various methods, namely electrochemical and plasma assisted polymerization techniques, can be employed for the fabrication of polyaniline thin films [11]. The composition, morphology and physical properties of the resulting polymers are strongly dependent on the method adopted for polymerization and reaction conditions.

Plasma polymerization is a novel and inexpensive technique for the fabrication of quality polymer coatings [12] and thin films [13]. Organic monomer vapours can be

[3] Author to whom any correspondence should be addressed.

polymerized at low temperatures using plasma treatment. This is a versatile technique to produce polymer thin films of organic compounds that do not polymerize under normal chemical polymerization techniques. Plasma polymer contains branched and randomly terminated chains with a high degree of cross linking. Chemical and electrochemical polymerization are the other two common methods used for obtaining polyaniline thin films. Although plasma polymer thin films lack the ordered and repeating units of monomer chains, they have a definite edge over other conventional polymerization techniques such as chemical and electrochemical polymerization techniques, plasma polymer thin films are pinhole free, chemically inert, thermally stable and are also of uniform thickness. Moreover, the composition of the plasma polymerized thin films can be tailored by appropriate processing conditions such as monomer flow rate, pressure in the chamber, deposition time and plasma power and can be suitably modified to get films with unique properties and which are unobtainable from the other polymerization techniques [13]. Moreover, the conductivity of the plasma polymerized thin films can also be tailored by *in situ* doping with appropriate dopants such as iodine and hydrogen chloride [13, 14]. The high adhesive nature of polymer thin films can find applications in anticorrosive surfaces, humidity sensors, electrical resistors and optical filters [14].

Doping of conducting polymers is normally resorted to for modifying the optical properties and is a unique, central and unifying theme of concept which distinguishes them from all other types of polymers [15]. The reaction of conducting polymers with iodine has historical importance and has led to a marked increase in the conductivity and modification of band gaps [6, 16, 17]. Although the halogenation of PANI using iodine and ring substitution of hydrogen atoms with iodine were reported [18–20], the effect of iodine on the conductivity and molecular structure is not well explored. Moreover, dopants such as iodine and acid groups have a profound influence on modifying the physical properties of PANI [10, 12] and so *in situ* doping of iodine during the synthesis of PANI thin films assumes importance in engineering the band gap of PANI thin films. The reasonably high power conversion efficiency and inexpensive nature of semiconducting polymers attracted the scientific attention in realizing polymer based photovoltaic cells and electronic displays [21]. The possibility for better charge injection, confinement and re-excitation makes heterostructures an ideal candidate for various devices such as solar cells and other optoelectronic devices [22]. Because of their higher efficiency, ordered polymer heterostructures are promising candidates in this regard [21]. Different methodologies have been adopted by different groups towards the realization of efficient polymer based photovoltaics and displays. Bulk heterostructures, ordered polymer heterostructures and polymer multijunctions are some of them [21]. Spin casting of the polymer and an electron acceptor from a common solvent is the common method for the fabrication of bulk heterostructures. The key challenge in making efficient polymer photovoltaics is the assurance of the intermixing of polymer and acceptor materials at a length scale of less than the exciton diffusion length for better efficiency [21]. Moreover, the efficiency of the bulk heterojunctions is also limited by the random network that is formed through the rapid drying of the solution during the spin casting process. Ordered polymer heterojunctions play an important role in this regard and various oxide–polymer tubular structures were synthesized. Different routes such as melt infiltration, dip coating and polymerization were adopted to fill the ordered inorganic oxide nanopores synthesized via different routes such as electrodeposition and tracked etching [21]. These organic–inorganic ordered nanostructures also lack efficiency and large area fabrication is not easily possible. Ordered organic–organic multijunctions are a viable alternative and the technique of RF plasma polymerization can be utilized to fabricate large area ordered structures. Scanning tunnelling microscopy/scanning tunnelling spectroscopy (STM/STS) is a versatile technique for investigating two-dimensional electronic systems in the nanometre scale [23] and can be used to study directly the electronic structure of nanometre scale polymer heterostructures.

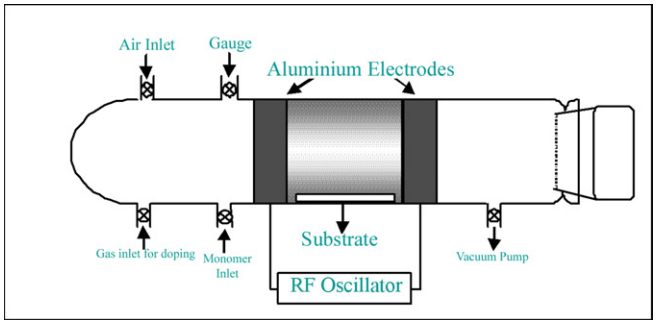

Figure 1. Schematic of RF plasma polymerization setup.

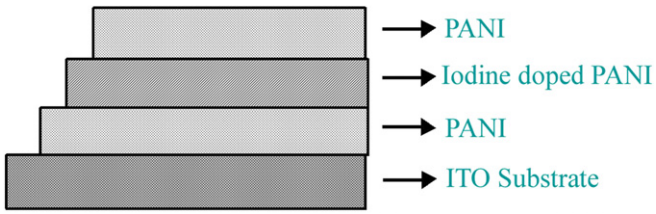

Figure 2. Schematic of P–I–P heterostructure geometry.

Here, we report the fabrication of polymer heterostructures based on polyaniline and iodine doped polyaniline using radio frequency (RF) plasma polymerization. The structural and electronic properties of these polyaniline–iodine doped polyaniline–polyaniline (P–I–P) heterostructures are studied using scanning electron microscopy (SEM), atomic force microscopy (AFM) and STM. The quantum well formation in these heterostructures is studied using room temperature STS.

2. Experiment

A home-made RF plasma polymerization unit (figure 1) was used for the fabrication of polymer thin films. Plasma polymerization unit consisted of a long glass tube of length 50 cm and of diameter ∼8 cm, with provisions for passing

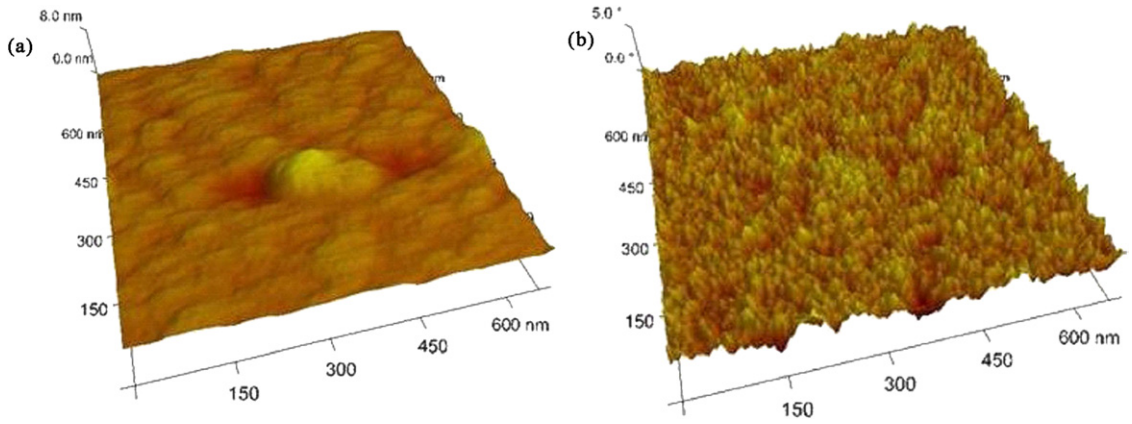

Figure 3. AFM image of polyaniline in (*a*) height mode and (*b*) phase mode.

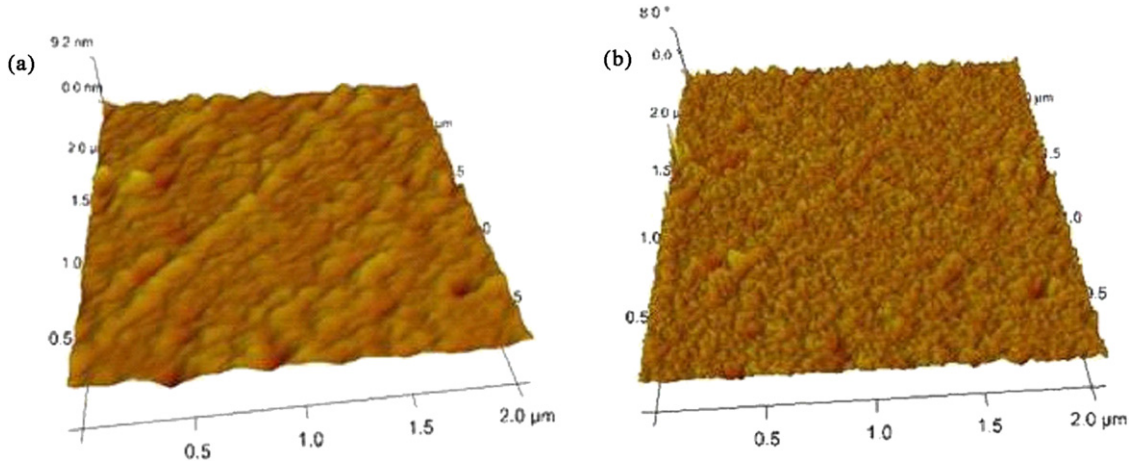

Figure 4. AFM image of iodine doped polyaniline in (*a*) height mode and (*b*) phase mode.

monomer vapour, dopants and for evacuation. The pressure in the chamber was maintained at $\sim 10^{-2}$ Torr.

An indium tin oxide (ITO) coated ultrasonically cleaned glass plate is used as the substrate for polymer deposition. Aluminium foils of 2 cm width were used as electrodes and the inter-electrode separation was kept at 5 cm. A glow of discharge was obtained in between the electrodes by applying a high frequency of 13 MHz and a current of 70 mA. Uniform cold nitrogen plasma having an average power of 20 W was maintained in between the two electrodes using an RF generator. A monomer (double distilled aniline) was evaporated into the plasma chamber at a monomer vapour pressure of 0.1 Torr and was deposited onto the ITO coated glass substrate. The deposition was continued for 3 min to obtain a polymer film of average thickness ∼40 nm. Proper masks were employed for the creation of heterostructures. The following geometry (figure 2) was chosen for the fabrication of P–I–P heterostructures.

The doping of iodine was carried out *in situ*, and it ensures the stability of iodine in the polymer matrix.

A Dektak 6M thickness profiler was used to determine the thickness and surface roughness of the polymer thin films. Fourier transform infrared spectroscopy (FTIR, Nicolet Avatar, 360 ESP-FTIR) was employed to identify the molecular structure and the presence of iodine in the polymer. AFM (Digital Instruments Nanoscope) studies were conducted to probe the surface morphology and roughness of the polymer thin films. A UV–Vis–NIR spectrophotometer (JASCO V-750) was employed to evaluate the band gap of thin films. SEM (JEOL, JSM-6390LV) and STM were used to identify the morphology of the heterostructures. STS studies were carried out using an STM tip and were used to map the local density of states in the polymer heterostructures. STM/STS studies were carried out using a Veeco-Digital Instruments multimode scanning probe microscope operated under ambient conditions. All the STM/STS studies reported here were performed using tungsten tips. The STM images were recorded in the constant current mode at a sample bias of 1.91 V and a current set point of 1.146 nA.

3. Results and discussion

Figures 3(*a*) and (*b*) show the AFM images of the polyaniline (pristine), PANI thin film, in the height mode and the phase mode, respectively. The average surface roughness is found to be 4.25 Å (film thickness calculated using the thickness profiler is ∼40 nm), which indicates that the formed PANI film is highly uniform. Figures 4(*a*) and (*b*) depict the AFM images of the iodine doped PANI (thickness ∼30 nm) thin film in the height

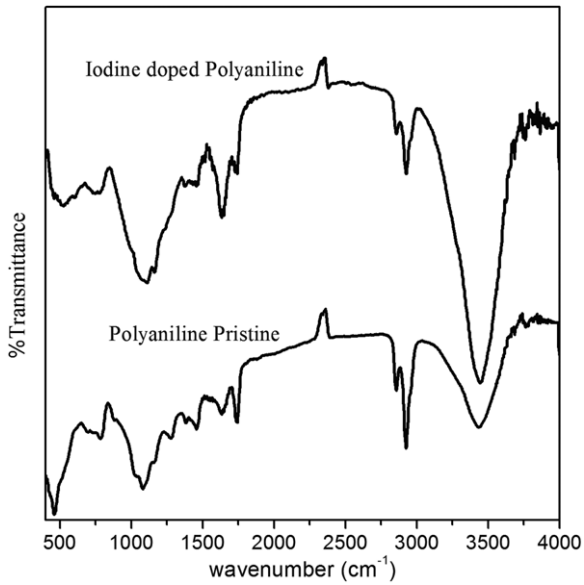

Figure 5. FT-IR spectrum of polyaniline and iodine doped polyaniline thin films.

Table 1. Frequency assignment of FT-IR spectrum.

Pristine polyaniline	Iodine doped polyaniline	Assignment of peaks
462.53		Out of plane ring bending vibration
694.21		C–H out of plane bending vibration, aromatic ring stretching
779.88	775.94	C–H out of plane bending vibration
878.09		C–H out of plane bending vibration
1076.86	1110.17	C–N stretching
1274.46	1164.22	C–N stretching, C–H in plane bending vibration
1382.85	1384.79	C–N stretching, aromatic ring stretching
1463.24	1461.83	N–H in plane bending vibration, aromatic ring stretching
1635.47	1641.24	C=C stretching, N–H in plane bending vibration
1740.89	1739.08	Overtones of C–H out of plane bending and combination bands
2853.85	2855.85	C–H stretching
2924.45	2925.74	C–H stretching
3435.36	3445.94	N–H stretching

and phase modes. The average surface roughness was found to be ∼4.51 Å.

The effect of iodine doping in the polymer structure is studied using an FT-IR spectroscope. Figure 5 shows the FT-IR spectrum of both the PANI and iodine doped PANI thin films.

The frequency assignment for FT-IR spectrum is carried out and is tabulated in table 1.

The FT-IR spectrum of iodine doped PANI shows the shifting of its peaks because doping with iodine modifies the bond length of the functional groups [2]. The intensity of the spectral peaks is also shifted in the doped sample. This indicates the structural difference between the doped and the undoped polyaniline thin films. The structural modification

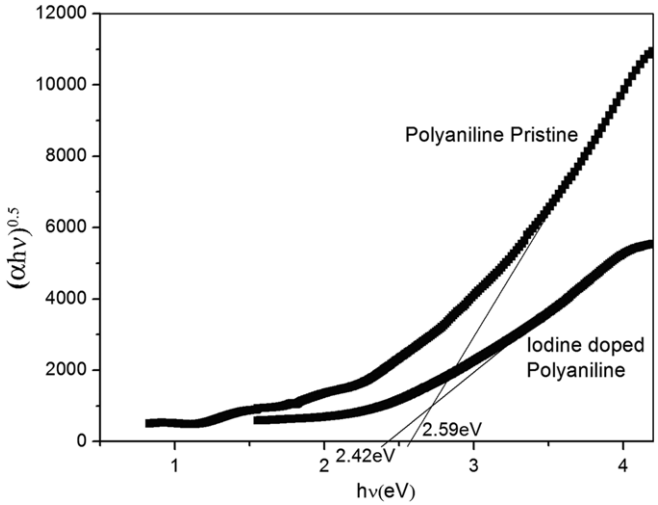

Figure 6. Band gap calculation for PANI and iodine doped PANI thin films.

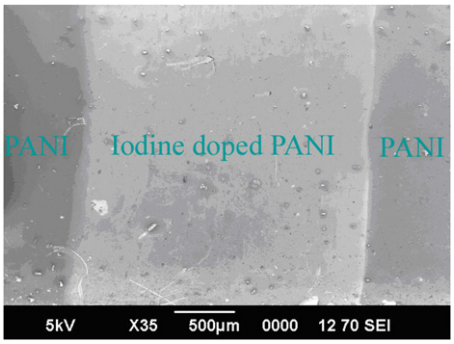

Figure 7. SEM image of P–I–P heterostructure.

due to the incorporation of iodine plays an important role in enhancing the conductivity of polyaniline [24]. The modification of the band gap in iodine doped PANI is further verified by measuring the UV–Vis absorption of both PANI and the iodine doped PANI thin films. Figure 6 shows the indirect band gap of PANI (pristine) and iodine doped PANI film derived from the Tauc relation [25].

The shift in the band gap of the iodine doped PANI film (∼0.2 eV) indicates the modification of the band gap of PANI with the doping of iodine.

The time of deposition was varied to get sandwiched heterostructures (deposition time for iodine doped PANI (middle layer) was 2 min and that of PANI was 3 min) and the other processing parameters were kept constant and they were as follows: plasma power 20 W, monomer vapour pressure 0.1 Torr, applied frequency 13 MHz and applied current 70 mA. Figure 7 shows the SEM image of the heterojunctions.

The difference in contrast in the middle portion is clearly visible in the microscope picture. The STM images and the line scan of the P–I–P heterostructure are shown in figure 8. The topographical images represent the height of the tunnelling tip above the sample. The images presented here are digitally filtered to remove the low frequency noises. The maxima in the STM image correspond to both topographical protrusions on the surface and increased local density of states.

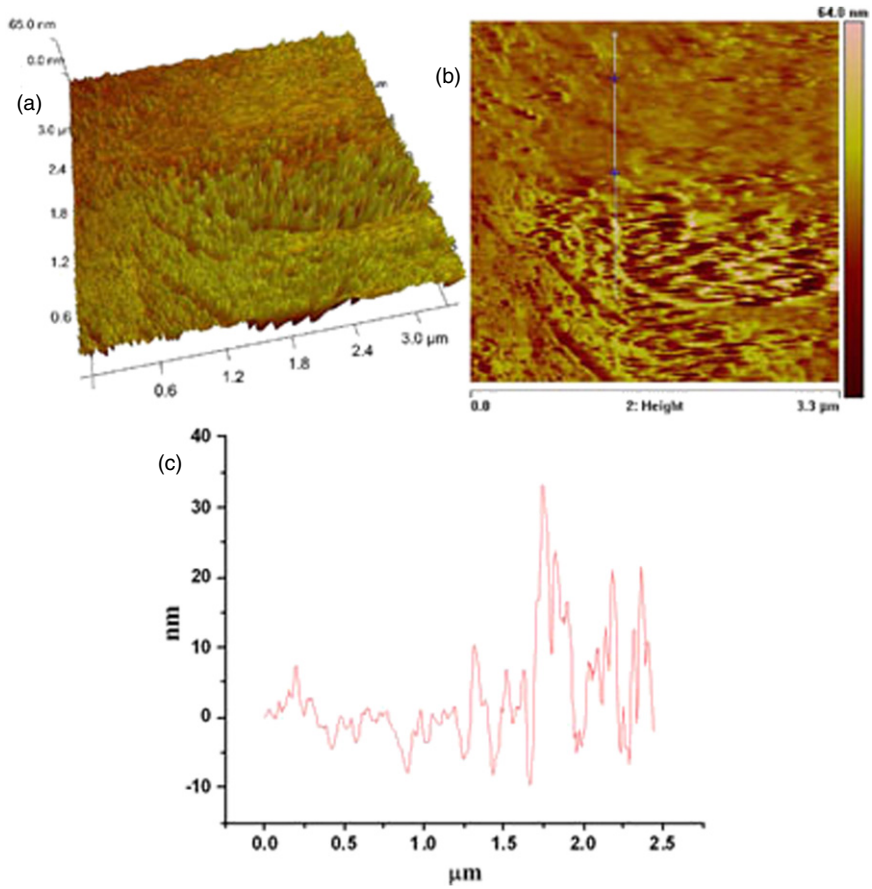

Figure 8. STM image of P–I–P heterostructure: (*a*) 3D view in constant current mode, (*b*) constant current mode and (*c*) line scan.

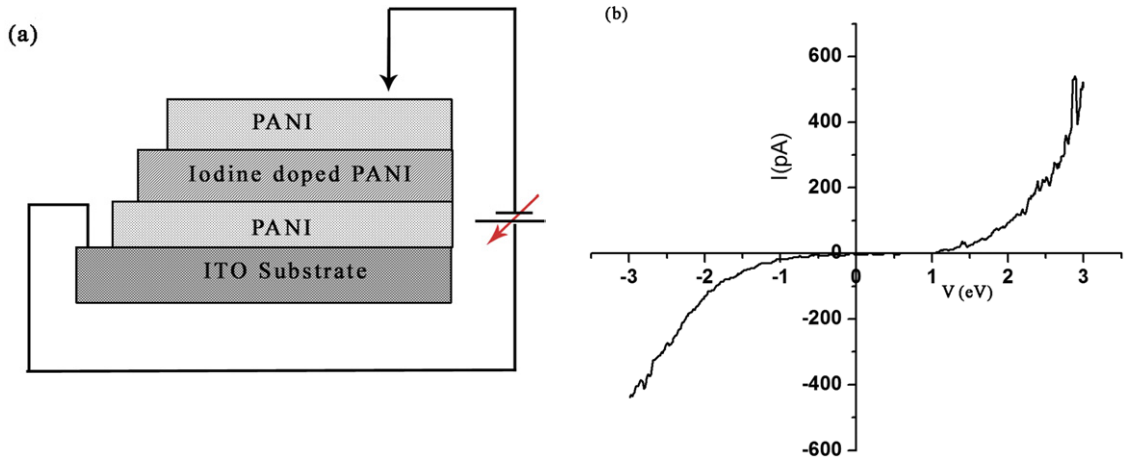

Figure 9. (*a*) Schematic of STS measurement and (*b*) $I(V)$ plot for P–I–P heterostructure.

STM image is taken from a $3\,\mu$m $\times$ $3\,\mu$m area of the sample. The STM image was recorded with an optimum value of tunnelling current of 1.146 pA and a bias voltage of 1.91 V in the constant current mode. Figure 8(*a*) represents the 3D STM image in constant current mode. Figure 8(*c*) represents the typical line scan carried across a heterojunction (P–I) through the marked portion in figure 8(*b*). The line scan indicates (figure 8(*c*)) that the thickness of the P layer is $\sim$30 nm, which is in agreement with that obtained from the thickness profiler for single films.

After achieving stable and repetitive STM images, the instrument was switched on to the STS mode to acquire the I–V characteristics. STS studies have been carried out to probe the local electronic density of states (LDOS) and the band gap of polymer surfaces at the nanometre scale. An STS measurement results in current versus voltage $I(V)$ characteristics, indicating the electronic structure at a specified (x, y) location.

Figure 9(*a*) shows the schematic of STS measurement by placing the STM tip over the PANI film and sweeping the

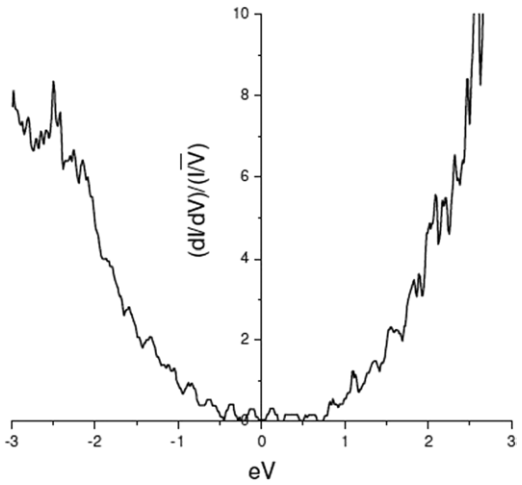

Figure 10. LDOS mapping for P–I–P heterostructure using STS.

bias voltage from −3 to 3 V, between the STM tip and the ITO substrate. Figure 9(*b*) depicts the $I(V)$ plot of the P–I–P heterostructure measured using STS.

The tunnelling current I is measured as the sample voltage V is ramped from −3 to 3 V. The spectral features manifest the density of states in the studied heterostructure [26]. The $\mathrm{d}I/\mathrm{d}V$ spectrum is normalized by the average conductance $(\overline{I/V})$ to cancel the exponential dependence of the tunnelling coefficient on V and the tip–sample separation and to avoid the divergence of $(\mathrm{d}I/\mathrm{d}V)/(I/V)$ at the band edge. So $(\mathrm{d}I/\mathrm{d}V)/(\overline{I/V})$ as a function of V is a good representation of the local density of states (LDOS) as a function of energy and is shown in figure 10.

The Fermi level is located at $V = 0$ eV. Below the Fermi level (negative voltage range) are the valence band states and the positive voltage represents the conduction band states. It is evident from figure 10 that LDOS in the conduction (or valence) band has a step-like energy dependence. The step-like energy dependence is due to the quantum confinement of electrons in the heterostructure and is a signature of quantum well-like confinement. The clear step-like energy dependence reveals the presence of sub-band states in the LDOS [27]. Normalized conductance at $V = 0$ eV provides a measure of the LDOS at the Fermi level, and it is found to be ∼0.037. This indicates a finite density of states at the Fermi level and formation of ordered nanoscopic structure in the P–I–P heterostructure [26]. Increase in the normalized conductance at the extreme voltages corresponds to the valence band and conduction band edges. The reported quantum well structures were those of semiconductors and they exhibited a step-like LDOS in the STS studies at much lower temperatures [27] and hence the quantum well confinement. Ruckh *et al* reported an energy band model calculation, based on the Huckel theory, for polydiacetylen (PDA) polyacetylen (PA) heterostructures [28]. These studies indicate that polymer superlattices can also behave like semiconductor heterostructures. These kinds of polymer quantum well structures are not only promising materials for various optoelectronic devices and displays but also offer a platform to investigate phenomena like quantum confinement and impurity state resonance.

4. Conclusions

A heterostructure based on polyaniline and iodine doped polyaniline (P–I–P) has been fabricated using RF plasma polymerization. The formation of heterostructure is verified using SEM and STM. The STS studies were carried out on the P–I–P heterostructure and the subsequent evaluation of LDOS confirmed the formation of quantum well heterostructures. This is presumably the first experimental report on the quantum well confinement in polymer heterostructures and these kinds of heterostructures can find applications in polymer based optoelectronic devices and sensors.

Acknowledgments

TNN acknowledges the Kerala State Council for Science, Technology and Environment (DO No 004/FSHIP/05/KSCSTE), Kerala, India, for financial support in the form of a fellowship. The authors thank STIC, CUSAT, for SEM measurements.

References

[1] Petty M C, Bryce M R and Bloor D (ed) 1995 *Introduction to Molecular Electronics* (Oxford: Oxford University Press) p 24
[2] Debangshu C, Suwarna D, Ranjani V and Sharma D D 2005 *Appl. Phys. Lett.* **87** 093117
[3] Jaroslav S, Miroslava T, Natalia V B, Elena N K, Stephanie R and Jan P 2008 *Polymer* **49** 180
[4] Andersson M R, Berggren M, Gustafsson G, Hjertberg T, Inganas O and Wennerstrom O 1995 *Synth. Met.* **71** 2183
[5] Albota M *et al* 1998 *Science* **281** 1653
[6] MacDiarmid A G 2001 *Angew. Chem. Int. Edn* **40** 2581
[7] Yan L and Gao Y L 2002 *Thin Solid Films* **417** 101
[8] Shu Q and Peng J-C 2008 *Chin. Phys. Lett.* **25** 3052
[9] Myeong H L, Gil S and Otto F S 2007 *J. Phys.: Condens. Matter* **19** 215204
[10] Wang H L, MacDiarmid A G, Wang Y Z, Gebler D D and Epstein A J 1996 *Synth. Met.* **78** 33
[11] Saravanan S, Joseph Mathai C, Anantharaman M R, Venkatachalam S, Avasthi D K and Singh F 2005 *Synth. Met.* **155** 311
[12] Sunny V, Narayanan T N, Sajeev U S, Sakthi Kumar D, Yoshida Y and Anantharaman M R 2006 *Nanotechnology* **17** 4765
[13] Saravanan S, Anantharaman M R, Venkatachalam S and Avasthi D K 2008 *Vacuum* **82** 56
[14] Saravanan S, Joseph Mathai C, Venkatachalam S and Anantharaman M R 2004 *New J. Phys.* **6** 64
[15] Chiang C K, Fincher C R Jr, Park Y W, Heeger A J, Shirakawa H, Louis E J and MacDirmid A G 1997 *Phys. Rev. Lett.* **39** 1098
[16] MacDiarmid A G 2001 *Rev. Mod. Phys.* **73** 701
[17] Sajeev U S, Joseph Mathai C, Saravanan S, Rajeev R A, Venkatachalam S and Anantharaman M R 2006 *Bull. Mater. Sci.* **29** 159
[18] Sahin Y, Percin S and Alsancak G O 2003 *J. Appl. Polym. Sci.* **89** 1652
[19] Berket G, Hue E and Sahin Y 2005 *Appl. Surf. Sci.* **252** 1233
[20] Gok A, Sari B and Talu M 2003 *J. Appl. Polym. Sci.* **89** 2823
[21] Mayer A C, Scully S R, Hardin B E, Rowell M W and McGhee M D 2007 *Mater. Today* **10** 28

[22] Valenzuella J and Milshtein S 2009 *Microelectron. J.* **40** 424
[23] Niimi Y, Kauisawa K, Kojima H, Kambara H, Hirayama Y, Tarucha S and Hiroshi F 2007 *J. Phys.: Conf. Ser.* **61** 874
[24] Saravanan S, Joseph Mathai C, Anantharaman M R, Venkatachalam S and Prabhakaran P V 2006 *J. Phys. Chem. Solids* **67** 1496
[25] Pankov J J 1972 *Optical Process in Semiconductors* (Englewood Cliffs, NJ: Prentice-Hall)
[26] Feenstra R M 1994 *Phys. Rev.* B **50** 4561
[27] Perraud S, Kanisawa K, Wang Z Z and Hirayama Y 2007 *J. Phys.: Conf. Ser.* **61** 926
[28] Ruckh R, Heine B and Sigmund E 1988 *Phys. Scr.* **38** 122